



## Halloysite Nanoclay-filled Blend Membranes of Sodium Carboxyl Methyl Cellulose/Hydroxyl Propyl Cellulose for Pervaporation Separation of Water-isopropanol Mixtures

K.V. Sekharnath<sup>1</sup>, U. Sajankumar ji Rao<sup>1</sup>, Y. Maruthi<sup>2</sup>, P. Kumar Babu<sup>2</sup>, K. Chowdoji Rao<sup>2</sup>, M.C.S. Subha<sup>1\*</sup>

<sup>1</sup>Department of Chemistry, Sri Krishnadevaraya University, Anantapur-515 003, Andhra Pradesh, India,

<sup>2</sup>Department of Polymer Science & Technology, Sri Krishnadevaraya University, Anantapur - 515 003, Andhra Pradesh, India.

Received 9<sup>th</sup> January 2015; Revised 04<sup>th</sup> March 2015; Accepted 08<sup>th</sup> March 2015

### ABSTRACT

Blend membranes of sodium carboxyl methyl cellulose/hydroxy propyl cellulose have been prepared by incorporating different amounts (5, 10 and 15 wt. %) of halloysite nanoclay (HNC) by solution casting method and cross-linked with glutaraldehyde. Membranes were characterized by fourier transform infrared spectroscopy, thermo gravimetric analysis, differential scanning calorimetry, X-ray diffraction and scanning electron microscopy, to confirm the chemical interactions and homogeneity of the blend membrane. The membranes prepared are used for pervaporation separation of water and isopropanol (IPA) mixtures at 30°C. In the studied feed composition range of 10-40 mass % of water; 15 mass % HNC loaded blend membranes gave the highest selectivity ranging between 2803.50 and 108.79, whereas the flux values increased from 0.364 to 0.442 kg/(m<sup>2</sup>h). The literature reviews show that, this is the first study of HNC filled sodium carboxymethyl cellulose/HPC blend membranes used in dehydration of IPA, which yield higher selectivity to water at higher loading of the clay as a filler.

**Key words:** Halloysite nanoclay, Pervaporation, Isopropanol/water, Flux, and selectivity.

### 1. INTRODUCTION

During the past decade or so polymer property modifications using nano particles and formation of nanocomposites has seen significantly of increased interest. There are several reasons why nanoparticles with dimensions on the nanometer scale (10<sup>-9</sup> m) are of interest. Nanoparticles with such small dimensions have been shown to improve not only the mechanical properties of the polymers but, in many cases, their functionalities as well [1-3]. In addition, only small loading of nanoparticles is sufficient to obtain significant property changes in membranes.

Halloysite nanotubes (HNTs) based on aluminosilicate clay nanosheets that are naturally rolled to form hollow tubular structures are mined from natural deposits [4,5]. While the ideal unit formula for halloysite is Al<sub>2</sub>Si<sub>2</sub>O<sub>5</sub>(OH)<sub>4</sub>.nH<sub>2</sub>O (n=0 for halloysite- [7Å] and n=2 for hydrated halloysite-[10Å]), the chemical composition is subject to variation due to the presence of impurities such as Fe oxides [5]. Halloysite has been found to occur widely throughout the world in weathered rocks as well as in soils and has been identified as

having formed by the alternation of a wide variety of igneous and non-igneous rocks [4-6]. It is often intermixed with dickite, kaolin, montmorillonite and other clay minerals [6]. Since the dominant morphology of halloysite is tubular, it is commonly termed as HNTs [5]. Unlike other nano structured clays that must be exfoliated, HNTs naturally occur as cylinders with average diameters typically smaller than 100 nm and lengths ranging from 500 nm to over 1.2 μm [6]. HNTs have been used as bioreactor, time-release capsules, catalysts of polymer degradation, templates for depositing other nanoparticles, polymer filler or property modifier as well as in ceramic applications [4]. HNTs have been widely used during recent years to reinforcing the polymer matrices such as epoxy resin, polypropylene, polyamide, styrene rubber and ethylene propylene diene monomer rubber [7-16]. Such nanocomposites, although show good mechanical and thermal properties, are not biodegradable and need to be disposed of in landfills at the end of their life [7-16]. In the case of biodegradable soy protein-based nanocomposites, the addition of HNTs was shown to improve their fire resistance [17].

\*Corresponding Author:

E-mail: mcssubha3@gmail.com

Purification of organic solvents, such as isopropanol (IPA) is widely used as a solvent in pharmaceutical industry as well as in many chemical processes such as acetone production, solvent extraction and in the manufacturing of hydrogen peroxide. High purity grade IPA is required as a cleansing agent in semiconductor and electronics industries [18-20]. Azeotropic composition of IPA with water is 12.2%, which makes it difficult to separate from water by the conventional distillation without recourse to carcinogenic benzene as an entrainer [21]. Alternatively, membrane-based pervaporation (PV) separation offers high separation efficiency along with high energy savings [22-25].

Sodium carboxymethyl cellulose (NaCMC) is carboxymethyl ether of cellulose, a well-known natural polysaccharide, comprising the fibrous tissue of plants. Hydroxyl groups on 2-glucopyranose residue of cellulose are replaced by carboxymethyl groups; the number of replacements is known as the degree of substitution (DS). Both DS and polymer chain length will determine solubility, viscosity, and gel strength of NaCMC. CMC, a natural, biodegradable anionic polymer with good biocompatibility, has been widely used in various fields ranging from technological industries to the biological, pharmaceutical, petroleum and medical fields, biomedical membrane [26-31].

Hydroxypropyl cellulose (HPC) is a cellulose derivative employed as coatings, excipients, encapsulations, binding materials, foaming agents, protection colloids, flocculants, and so forth, for a wide variety of applications in food, drugs, paper, ceramics, plastics, and so forth [32]. HPC films are used as a food additive; HPC is used as a thickener, a low-level binder and as an emulsion stabilizer with E number E463. In pharmaceuticals, it is used as disintegrate, and a binder, in tablets [33]. They act as acceptable barriers to moisture and oxygen [34,35]. Blends based on HPC with natural or synthetic polymers were proposed to design new materials with enhanced properties and with a wide range of applications. Moreover, NaCMC can interact strongly with HPC. Consequently, NaCMC/HPC blend membrane with good mechanical property is prepared using glutaraldehyde (GA) as crosslinking reagent was widely investigated in the fields of PV separation in water-ethanol mixture, separator in electro-generation, antiadhesion after operation [36,37]. However, usage of NaCMC/HPC membranes in PV was not found in the literature.

On the basis of the above consideration, NaCMC/HPC membranes are expected to develop to be used as PV membrane. In this study, an effort has been made to enhance the flux and separation selectivity simultaneously by judiciously choosing halloysite nanoclay (HNC) and incorporation of it into NaCMC/HPC matrix. The clay content with respect to NaCMC

and HPC was varied in the range of 5-15% with the aim of improving membrane performance. The physicochemical changes in the resulting membranes were investigated, and the resulting membranes were used for the PV separation of water/IPA mixtures at different concentrations of water (10-40%) in water/IPA [38]. The results of permeation flux, separation selectivity, and diffusion coefficients were evaluated. The results were discussed in terms of swelling properties of the membranes.

## 2. EXPERIMENTAL

### 2.1. Materials

NaCMC (viscosity [1W/V %], 1100-1900 cps) was purchased from Merck, Mumbai, India, HPC (M/W:80,000) and HNC were purchased from Sigma-Aldrich (USA), GA, hydrochloric acid (HCl), isopropyl alcohol, and acetone are of analytical grade purchased from Sd. Fine-chem. limited (India). HNC was purchased from Aldrich Chemical Company, Milwaukee, WI, USA. Double-distilled water collected in the laboratory was used throughout this research work. All the chemicals were used as received without further purification.

### 2.2. Preparation of Membrane

NaCMC and HPC (2 g each) was dissolved in 90 mL distilled water separately under constant stirring (Remi Equipment Model 2 MLH, Mumbai, India) for about 24 h at room temperature. Separately, the 5, 10, and 15% of HNC particles was dispersed in 10 mL DI water by sonication for 2 h. This was added to the previously prepared NaCMC/HPC (50:50) blend solution and then the whole mixture was kept under stirring for another 24 h. The blend solution was poured on to a prelevelled glass plate in dust-free atmosphere to cast the membranes with uniform thickness. Membranes thus formed were allowed to dry at ambient temperature and then peeled-off from the glass plate and then cross-linked with GA (2.5 mL) containing 85:10 acetone/water mixture in which 2.5 mL HCl was added as activator and allowed for cross-linking reaction for 12 h. Acetone being a non-solvent prevents the initial dissolution of the membrane and water present in the feed leading to swell the membrane there by facilitating an easy penetration of GA into the membrane matrix for an effective crosslinking. Crosslinking reaction takes place between the OH groups of NaCMC, HPC, and CHO groups of GA because of the formation of ether linkages by eliminating water molecules.

The cross-linked membranes were removed from crosslinking bath and washed repeatedly with distilled water to remove the adhered GA and unreacted molecules and then dried in hot air oven at 40°C to content weight and the membrane. The membranes containing different amounts of HNC, i.e., 5, 10 and 15% were designated as M1, M2, and M3, respectively.

Plain NaCMC/HPC (50:50) blend membrane (without clay) was prepared in same process as described earlier, and it was designed as blend membrane thickness was measured using micrometer screw gauge, and the thickness for the membranes was found to be around 35-40  $\mu\text{m}$ . Membrane's thus prepared were used for further characterization and for dehydration of IPA/water mixture (90:10, 87.5:12.5, 85:15 and 82.5:17.5). Clay loading was limited to 15 wt% because beyond this concentration membrane becomes brittle.

### 2.3. Membrane Characterization

The presine, crosslinked and halloysite nanoclay loaded membranes have been characterized by different techniques such as FTIR, DSC, XRD and SEM.

### 2.4. Fourier Transform Infrared (FTIR) Spectroscopy

FTIR spectra of HPC, NACMC, and their blend films were taken using Bomem MB-3000, Canada. The membranes are finely grounded with KBr to prepare the pellets under a hydraulic pressure of 600 dynes/m<sup>2</sup> and spectra were scanned between 4000 and 400 cm<sup>-1</sup>.

### 2.5. Differential Scanning Calorimetry (DSC)

DSC curves of HPC, NACMC, and their blend films of different compositions were recorded using TA instruments DSC (Model: SDTQ-600, USA). The analysis of samples was performed at the heating rate of 20°C/min under N<sub>2</sub> atmosphere at a purge speed of 100 mL/min.

### 2.6. X-Ray Diffraction (XRD)

The XRD patterns of the blend samples were obtained with an Intel diffractometer (Paris, France) with monochromatized Cu K $\alpha$  radiation (scan speed of 0.6°/min in a 2 $\theta$  range of 5°–40°) at room temperature.

### 2.7. Scanning Electron Microscope (SEM)

SEM micrographs of the membranes were obtained under high resolution (Mag 300  $\times$  5 kv) Using Leo Model Leica-stereoscan 440, SEM, equipped with phoenix energy dispersive analysis. SEM micrographs were taken at South Korea.

### 2.8. Swelling Studies

Equilibrium swelling of the membrane was performed gravimetrically at 30°C in 10, 12.5, 15, 17.5 wt% water containing feed mixtures as well as pure water and pure IPA. Initial masses of the circularly cut (diameters = 2.5 cm) nascent blend NaCMC/HPC membrane and MMMs were measured on a single-pan digital microbalance (Model ADAM AFP-210L.) accuracy to 10<sup>-4</sup> g. Dry membranes were placed inside the specially designed airtight test bottles in 20 cm<sup>3</sup> solvent media, equilibrated overnight to attain maximum swelling and the swollen membranes were removed from the bottles to weigh them immediately on a microbalance after carefully blotting with soft papers. The equilibrium swelling, DS, was then calculated using

$$DS\% = \left( \frac{W_s - W_d}{W_d} \right) \times 100 \quad (1)$$

Where, W<sub>s</sub> and W<sub>d</sub> are weights of the swollen (at equilibrium time) and dry membranes (at initial zero time), respectively.

### 2.9. PV Dehydration Experiments

PV dehydration experiments were performed at 30°C using a previously designed apparatus [39] that has an effective membrane area of 28.27 cm<sup>2</sup> and liquid volume of 250 cm<sup>3</sup>. The apparatus was made of a stainless steel cell in which the feed stock solution was maintained at the desired temperature by a thermostatically controlled water jacket. An efficient three-blade stirrer powered by a DC motor was used in the feed compartment for stirring the mixture at 200 rpm and maintaining a down-steam pressure of 0.5 mmHg using a vacuum pump (Model: BD-53, WTB Binder, Tuttlingen, Germany).

Before the actual measurement, the test membrane was equilibrated for 3 h with the feed mixture at ambient temperature. After establishment of a steady state, permeate was collected, condensed in traps using liquid nitrogen for up to 3–4 h, the flux was calculated by weighing the permeate on a digital microbalance (model AFP 210L) and its composition was determined by measuring its refractive index by comparing it with the standard graph of refractive index versus mixture composition of the feed system. The selectivity of a given membrane was estimated using the following equation [40]

$$J_p = W_p / At \quad (2)$$

Here, W<sub>p</sub> represents the mass of water in permeate (kg); A is the membrane area (m<sup>2</sup>) and t represents the permeation time (h),

$$\alpha = \left( \frac{Y_A}{1 - Y_A} \right) \left( \frac{1 - X_A}{X_A} \right) \quad (3)$$

Where, X<sub>A</sub> is wt% of water in the feed and Y<sub>A</sub> is wt% of water in the permeate.

At least three independent measurements of flux and selectivity were made under the same conditions of temperature and feed composition to confirm the steady-state PV.

## 3. RESULTS AND DISCUSSION

Scheme 1 represent the polymers used in the study and also shows the structure of NaCMC/HPC blend cross linked with GA, where the CHO groups of GA, react with the hydroxyl groups of NaCMC/HPC resulting in the formation of covalent bond. This can also be

confirmed by FTIR Studies. It was noticed that both the homo-polymers and the NaCMC/HPC blends optically clear to the naked eye. No separation into two layers or any precipitation was noticed when allowed to stand for 1 month at room temperature.

**3.1. FTIR**

The FTIR spectra of pure HNC, pure NaCMC/HPC blend membrane (M0) and its blends of various formulations containing different amounts of HNC 5, 10, and 15 wt% (M0, M1, and M2) are illustrated in Figure 1.

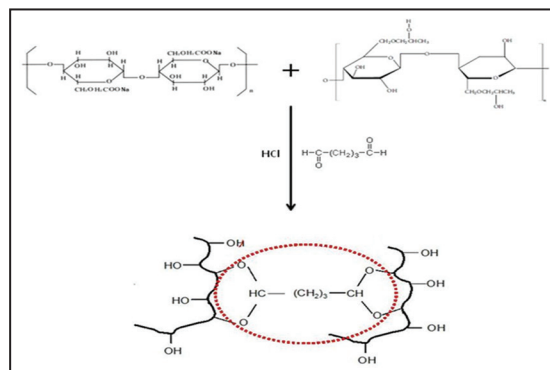
From Figure 1, for pure HNC spectra, it is observed that the absorption bands at 3,695 and 3,620  $\text{cm}^{-1}$  were assigned to the stretching vibration due to the inner-surface of O-H groups of halloysite, respectively. The interlayer water is indicated by the vibration at 1,647  $\text{cm}^{-1}$ ; the 1,111  $\text{cm}^{-1}$  peak was assigned to the stretching mode of Si-O while the band at 1,030  $\text{cm}^{-1}$  was caused by the stretching vibration of Si-O-Si. The band observed at 538  $\text{cm}^{-1}$  was due to the vibration of Al-O-Si. The vibration of the inner-surface hydroxyl group at 912  $\text{cm}^{-1}$  and Si-O-Si at 520  $\text{cm}^{-1}$  confirm the existence of corresponding groups. The bands observed in the halloysite showed no significant changes, since the majorities are assigned to Si-O and Al-O bonds.

A characteristic strong and broadband exhibited around 3440  $\text{cm}^{-1}$  in M0 membrane, corresponds to O-H stretching vibrations of NaCMC and HPC. Bands at 2937 and 2907  $\text{cm}^{-1}$  indicates aliphatic C-H stretching vibrations, peaks at 1604 and 1425  $\text{cm}^{-1}$  are due to asymmetric and symmetric stretching of carboxylate groups of NaCMC, whereas peaks observed at 1120 and 1028  $\text{cm}^{-1}$  represents C-O-C stretching vibrations [41]. In the case of cross-linked M0 membrane, a new peak at 1248  $\text{cm}^{-1}$  was observed due to the formation of ether linkage on crosslinking NaCMC/HPC membrane with GA (Figure 1). In clay-filled membranes, in addition to the peaks observed in Mo, a new peak was observed at 956  $\text{cm}^{-1}$  due to Si-O-Si group of HNC. From the above figure it is also observed that as the clay content increases the intensity of the peaks did not alter, instead the peaks shifted to lower wavelength for membranes containing 5-15 wt% clay (curves M1, M2 and M3). This is due to the increase of Si-O-Si groups of HNC which appear almost at the same frequency of C-O stretching. All these evidences ascertain the increase of clay incorporation in the membrane matrix.

**3.2. DSC**

DSC thermograms of cross-linked NaCMC/HPC blend membrane (M0) and its blends of two formulations containing different amounts of HNC 5 wt% (M1) and 10 wt% (M2) are shown in Figure 2, respectively.

From the DSC curves of the unfilled (M0) and filled (M1, M2) matrix membranes shown in Figure 2. M0 reveals a relatively large and sharp melting endothermic peak at 223°C. On the other hand,



**Scheme 1:** Schematic diagram showing the interaction between GA and NaCMC/HPC blend.

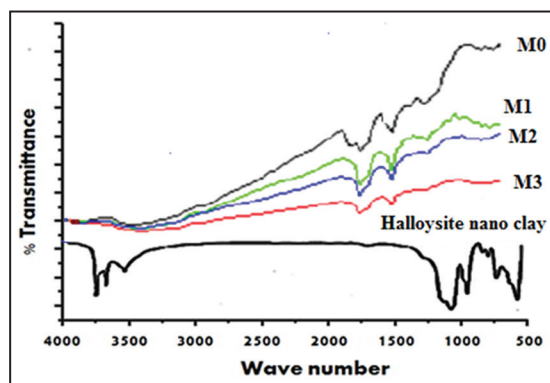


**Figure 1:** Fourier transform infrared spectra of M0: without clay incorporated blend membrane, M1: 5 wt% clay incorporated blend membranes, M2: 10 wt% clay incorporated blend membrane, and M3: 15 wt% clay incorporated blend membrane.

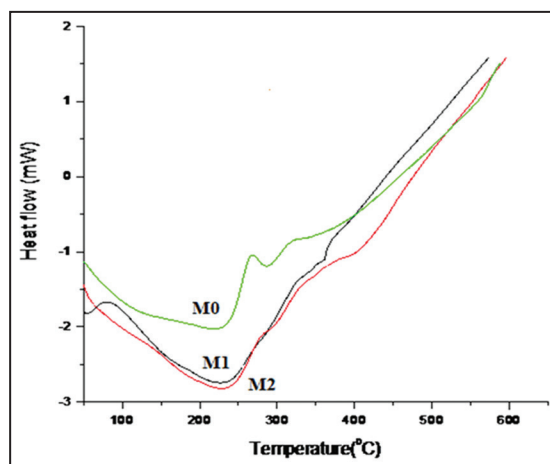


**Figure 2:** Differential scanning calorimetry thermograms of (a) M0: NaCMC/HPC blend and (b) M1: Blend incorporated with 5 wt% of clay (c) M2: blend incorporated with 10 wt% of clay.

weak and broad melting endothermic peaks of blend segments in the mixed matrix membranes appeared at higher melting point, i.e., around 250°C. As the content of clay increased, the endothermic curve of blend segments became broader, and its peak shifted to higher temperatures. The increase of the melting temperature and the peak broadening indicates that the ordered association of the blend molecules was increased by the presence of HNC, which is due to their inorganic nature.

### 3.3. Thermo Gravimetric Analysis (TGA)

The results of TGA of pure NaCMC/HPC blend membrane (M0) and blend membranes containing different amounts of HNC (M1 and M2) are shown in Figure 3.

Thermal stability of the clay embedded mixed matrix membranes was analyzed by using TGA. The TGA curves of the plain blend (M-0), M-1 and M-2 are shown in Figure 3. It can be observed that first weight loss event occurs just above 100°C for all the samples. This weight loss is attributed to the loss of water molecules. In the plain blend membrane, the major mass loss took place from about 230-290°C and was followed by a further smaller mass loss from about 290-490°C. On other hand, M-1 and M-2 showed two weight loss stages one at in the range 220-280°C, and further 2<sup>nd</sup> followed in the range 280-480°C. Mixed matrix membranes had a quite similar changing tendency to pristine blend membrane, which indicated that incorporation of clay into blend improves the thermal stability of the membranes. TGA studies indicate that the mixed matrix membranes can be effectively used in PV experiments at temperature up to 150°C temperature. Further, it is observed from Figure 3 that the thermal stability is in the following order, i.e., M2 > M1 > M0, which is due to the intercalation of blend membranes with inorganic clay.

### 3.4. XRD

The XRD patterns of the plain blend NaCMC/HPC, clay loaded formulations M1 and M2 are presented in Figure 4. The pristine blend membrane (M0) exhibits crystalline peaks at 12°, 30°, 37°, 39°, 42°, 48°, and 58°. However the clay loaded blend membranes (M1 and M2) show all the crystalline peaks of M0 and also show additional peaks, which are characterization peaks of HNC. Clay filled blend membranes M1 (5 wt%) and M2 (10 wt%) have shown more crystalline nature compared to M0. On increasing the clay content (5-10%) in the membrane matrix, the intensity of the clay peaks increased marginally, suggesting the increase in its crystallinity. This is attributed due to the increase of clay content responsible for bond formulation between clay particles and the membrane matrix, morphological studies (in this study) also reveals similar results.

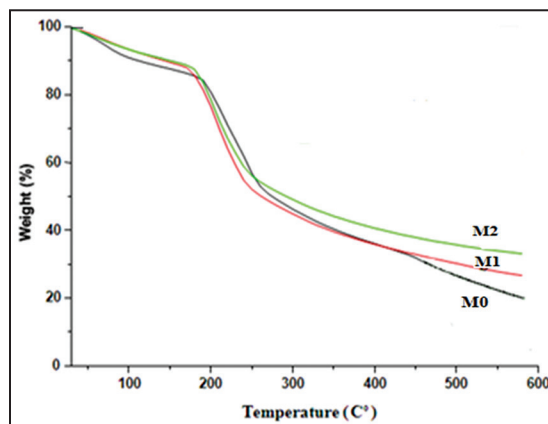


**Figure 3:** Thermo gravimetric analysis curves of (a) M0: NaCMC/HPC pristine blend and (b) M1: blend incorporated with 5 wt% of clay (c). M2: blend incorporated with 10 wt% of clay.

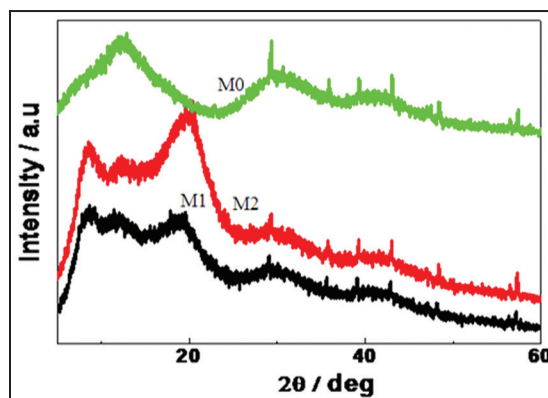


**Figure 4:** X-ray diffraction of the (M0) blend membrane and (M1) blend incorporated 5 wt% of clay, (M2) blend incorporated 10 wt% of clay.

### 3.5. SEM

SEM is a widely used technique to study morphology and surface characteristics of the materials. In the present study, SEM is used to assess morphological change in modified blend, for various combination of NaCMC/HPC/HNC that were recorded and presented in Figure 5.

Figure 5 represent the SEM micrograms of surface morphology of the pristine NaCMC/HPC (M0) and its clay incorporated membranes (M1, M2, and M3). The micrograms confirm that the clay distribution increased from membrane M1 to M3 with increasing clay loading. The clay was distributed evenly throughout the NaCMC/HPC matrix this would help to facilitate an easy transport of water molecules through the membranes [42], but when the clay content reaches 15%, part of the clay aggregate at the interface of the membrane, which could be disadvantageous for PV performance. Furthermore, the micrograms clearly show that the clay crystals were embedded in the membrane matrix, with no voids around them up to

10% clay content in the membrane. This ensured that the clay incorporated membranes obtained here were free from possible defects up-to 10% HNC.

### 3.6. Swelling Results

From the sorption studies, the amount of water responsible for swelling the membranes was investigated at different compositions of IPA-water mixtures. The overall % degree of swelling was computed using equation (1), and the results are presented in Table 1. The results indicate that the degree of swelling behavior of a preferential component affects the PV membrane performance. This property depends on the nature of membrane material and the membrane preparation conditions. The variation of degree of swelling of the pure blend membrane (M0) and the mixed matrix membranes (M1, M2, and M3) with wt% of the feed are shown in Figure 6.

Swelling experiment has significance in the study of interactions between permeant molecules and the membrane matrix as well as to understand the effect of filler loading on the sorption characteristics of the membrane. Dynamic and equilibrium swelling experiments on the plain NaCMC/HPC blend membrane, and mixed matrix membranes were carried out at different feed water- IPA compositions at 30°C.

From the Table 1 and Figure 6, It is clearly seen that for pure blend membrane (M0) and HNC filled NaCMC/HPC blend membranes (M1, M2, and M3), the degree of swelling of the membranes increases with increasing water concentration in the feed solution. By comparison, the mixed matrix membranes have a degree of swelling lower than that of unloaded blend membrane. Modification of the NaCMC/HPC mixed matrix membranes via chemical crosslinking resulted in a more compact structure and, therefore, the membrane acquire less affinity and less swelling ability.

### 3.7. Membrane Performance Through PV Studies

The results of PV performance in terms of feed composition, permeate composition, selectivity, flux and PV separation index (PSI) are given in Table 2. The efficiency of the membranes in PV process is generally assessed based on the permeation of individual components. Therefore, the extent of permeation was determined by plotting the flux of water as a function of clay content in the membrane for 10-40 mass% of water in the feed.

### 3.8. Membrane Performance on Flux and Selectivity

Membrane performance of pristine blend membrane (M0) and Mixed matrix membranes (M1, M2, and M3) have been studied by calculating flux, selectivity, permeation and separation index (Table 2). In PV, molecular transport occurs due to the concentration gradient that exists between feed and permeate sides of the membrane; this process is generally explained

**Table 1:** Percentage of swelling data of blend membranes in different water in the feed/IPA mixtures at 30°C.

% of water in the feed	% of swelling			
	M0	M1	M2	M3
10.0	39.2	31.25	21.1	18.3
12.5	44.8	42.48	27.5	27.0
15.0	50.2	48.90	44.8	42.9
17.5	57.0	54.00	53.1	44.6

IPA: Isopropanol

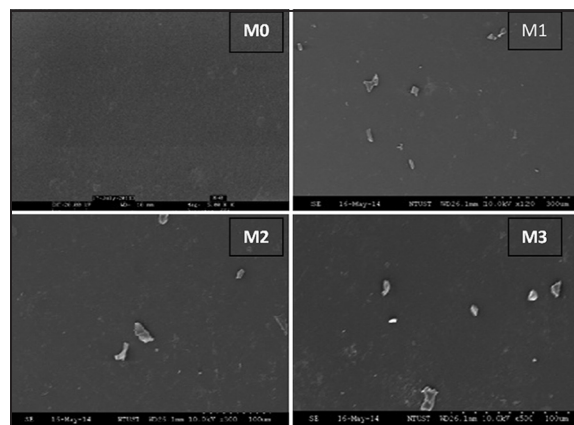


**Figure 5:** Scanning electron microscope images of (M0): pristine blend membrane, (M1): blend incorporated with 5 wt% of clay, (M2): blend incorporated with 10% of clay, (M3):blend incorporated with 15% of clay.

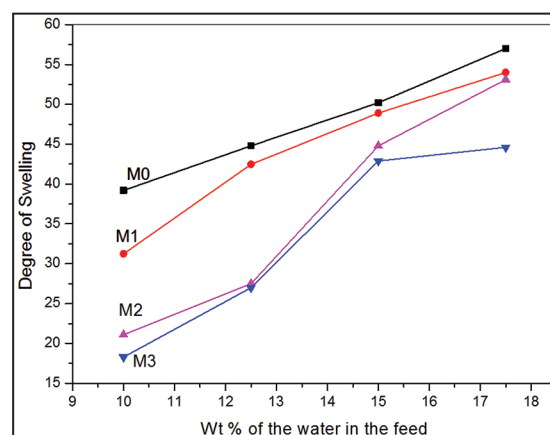


**Figure 6:** Effects of feed water content on degree of swelling of different mixed matrix membranes.

by the solution- diffusion mechanism. According to this principle, permeating molecules first dissolve in the membrane and then diffuse out as a consequence of the concentration gradient. However, the overall separation can be explained on the basis of the physical nature of the solvents, their affinity towards membrane as well as the morphological set up of the membrane. It is well-known that IPA can diffuse into the blend

**Table 2:** PV data of IPA/water mixtures for different membranes at 30°C.

Feed compositions		Permeate compositions (wt%)		Selectivity ( $\alpha$ )	Flux ( $\text{kg/m}^2\text{h}$ )	PSI
Water (x)	IPA (1-x)	Water (y)	IPA (1-y)			
M-0 (50:50)						
10	90	98.89	1.11	801.81	0.364	291.49
20	80	98.54	1.46	289.82	0.398	114.95
30	70	98.42	1.58	122.15	0.409	49.55
40	60	97.82	2.18	67.30	0.418	27.97
M-1 (5%)						
10	90	99.32	0.68	1314.52	0.122	160.24
20	80	98.84	1.16	344.27	0.146	50.11
30	70	98.52	1.48	155.32	0.167	25.77
40	60	98.24	1.76	83.72	0.180	14.88
M-2 (10%)						
10	90	99.54	0.46	1947.52	0.228	443.80
20	80	99.32	0.68	584.23	0.240	139.97
30	70	98.82	1.18	195.40	0.262	50.93
40	60	98.44	1.56	94.65	0.288	26.97
M-3 (15%)						
10	90	99.68	0.32	2803.50	0.364	1020.11
20	80	99.38	0.62	641.16	0.384	245.82
30	70	98.92	1.02	226.42	0.402	90.61
40	60	98.64	1.36	108.79	0.442	44.84

IPA: Isopropanol, PV: Pervaporation, PSI: Pervaporation separation index

matrix due to hydrophilic-hydrophilic interactions. However, after adding HNC swelling of blend membrane is controlled, which will give a decrease in the diffusive transport of organic molecules since selectivity to water increases, depending upon the clay content in the mixed matrix membrane, performance will change. NaCMC/HPC blend membrane had many hydroxyl groups and was very tight membrane that is caused by the high degree of inter-and intra-molecular hydrogen bonding effects.

### 3.9. Effect of Feed Composition on PV Results

Pristine NaCMC/HPC blend membrane has a large number of hydroxyl groups and hence, it sorbs to a greater extent upon contact with hydrophilic water, thus, rendering the NaCMC/HPC blend membrane mechanically weak for performing the PV experiments. Therefore, it is necessary to prepare blend membranes that can be used in PV dehydration studies of water-organic feed mixture by blending, grafting, MMMs, etc. [38,43-45]. In the present investigation, it is demonstrated that by incorporating clay particles, one can improve the solvent stability of blend membrane, thus, increasing the membrane performance. As presented in Figure 7a, flux values of a mixed blend matrix membrane (M1, M2, and M3) are slightly lower than those of the pristine

blend membrane (M0). For NaCMC/HPC/HNC mixed matrix membranes, flux values increased with increasing feed water composition from 10 to 40 wt%. However, even at lower amount of water, i.e., 10 wt% of the feed mixture, there is a strong tendency of water molecules to get adsorbed onto HNC layers. At higher concentration of water in the feed mixture, water will exert the induced plasticization effect to NaCMC/HPC. For M3 membrane, from Figure 7b it is observed that the selectivity for water-IPA is 2803.50 at 10 wt% of water in the feed which decreased with increasing concentration of water in the feed (Figure 7b). At higher concentration of water in the feed mixture, M3 membrane could absorb more amounts of water molecules when compared to pristine blend membrane, M1 membrane due to plasticization effect of the polymer. However, selectivity has decreased, but the flux decreased considerably at 15 wt% clay containing blend membrane. For 40 wt% water containing feed mixture, selectivity decreased to 108.79, but the flux was enhanced to 0.442  $\text{kg/m}^2\text{h}$  for the M3 membrane. In case of M0, M1 and M2 membrane, the respective values for 40 wt% water contains feed mixtures are much lower, i.e., 67.30, 0.418  $\text{kg/m}^2\text{h}$ , 83.72, 0.180  $\text{kg/m}^2\text{h}$  and 94.65, 0.288  $\text{kg/m}^2\text{h}$ . In all cases, flux and selectivity of blend-clay membranes are higher than that of M0. In any case, the present

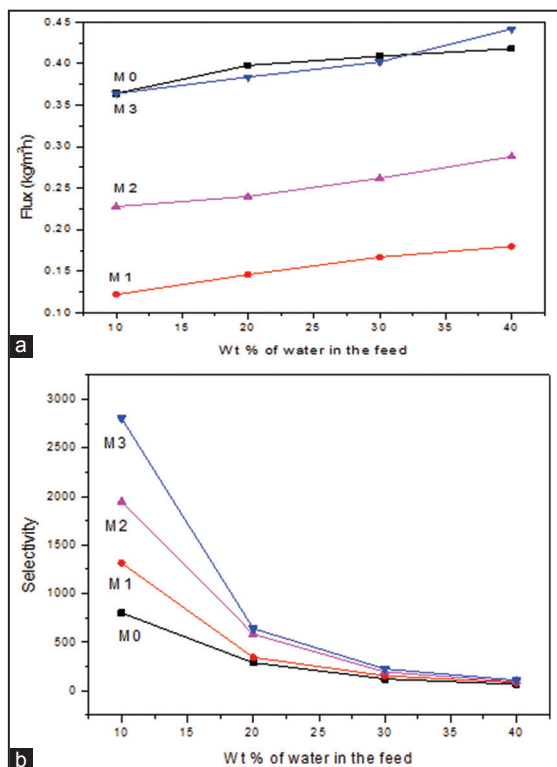


**Figure 7:** (a) Effect of wt% of water in the feed on flux for different formulations, (b) Effect of wt% of water in the feed on selectivity for different formulations.

study demonstrates the positive role played by HNC upon incorporation into NaCMC/HPC to enhance the membrane performance over that of pristine cross-linked NaCMC/HPC membrane.

### 3.10. Effect of PSI

The PV results have been discussed in terms of PSI at 30°C as shown in Figure 8 at 30°C as given in Table 2. PSI values decrease systematically with increasing water concentrations of the feed mixtures. The values of PSI are higher for the M3 mixed matrix membrane when compared to M2 and pristine blend membrane (M0).

### 3.11. Effect of HNC Content on PV Performance

The variations of flux and selectivity are studied as a function of different wt% of HNC particles into blend membrane.

From the Table 2 it is noticed that the pristine blend membrane exhibited a selectivity of 801.81 with a flux of 0.364 kg/m<sup>2</sup>h at 10 wt% of water in the feed mixture of IPA. Selectivity of blend membrane increased after the incorporation of HNC particles. At 10 wt% of water in the feed mixture for M1 membrane, the selectivity and flux were increased to 1314.52 and 0.122 kg/m<sup>2</sup>h respectively, while that for M2 membrane, the values were 1947.52 and 0.228 kg/m<sup>2</sup>h, and further for M3 membrane the selectivity and flux values were increased to 2803.50 and 0.364 kg/m<sup>2</sup>h. However

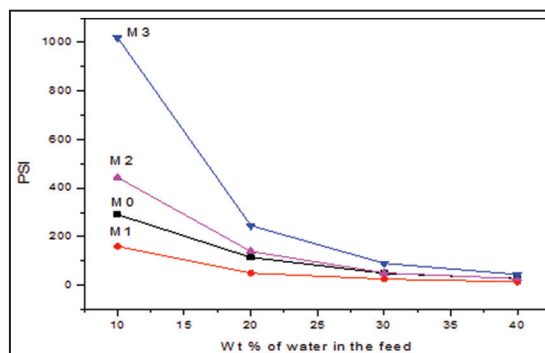


**Figure 8:** Effect of wt% of water in the feed on PSI for different formulations.

this favors the molecular level interaction between the polymer and the clay, resulting in decreased free volume. In addition, a high aspect ratio of layered silicates caused them to act as a barrier, offering more resistance to diffusion by creating tortuosity to the diffusion pathway. This has suppressed the diffusion of both water and IPA molecules. However, the diffusion of IPA molecule was affected significantly as the kinetic diameter of IPA molecule is almost four times bigger than that of the water molecule [46]. Obviously, transport of IPA molecules was less preferred as compared to water molecules, resulting in increased selectivity and decreased permeation flux. On further increase of the amount of clay beyond 10 wt% of water in the feed mixture fluxes is decreased. The decrease in flux accounted for the lower degree of swelling at higher mass % of HNC. These increased values with increasing loading of clay compared to the blend membrane (M0) can be attributed to the fact that clay provides higher hydrophilicity and higher strength to the blend membrane. The simultaneous increase of selectivity and flux is a difficult problem in PV separation, even though several studies have demonstrated this effect [47,48]. From the plot of selectivity and flux vs filler loading shown in Figure 9a and b, we came to know that selectivity and flux increased with filler loading suggesting suitability of the composite membrane for interchanging phenomena.

Since both blend membrane and clay particles are hydrophilic in nature and, therefore, membrane performance can be explained on the basis of solution-diffusion theory in addition to adsorption-desorption concepts [49]. In blend membrane (M0), the permeating water molecules first get absorbed into the microvoids and then diffuse out on the permeate side due to the existence of the concentration gradient. In the case of filled matrix membranes, the overall separation can be explained by the hydrophilic interactions between clay particles and the blend membrane. The clay particles may be distributed throughout the blend membrane, thus, forming a strong intercalation. However, majority



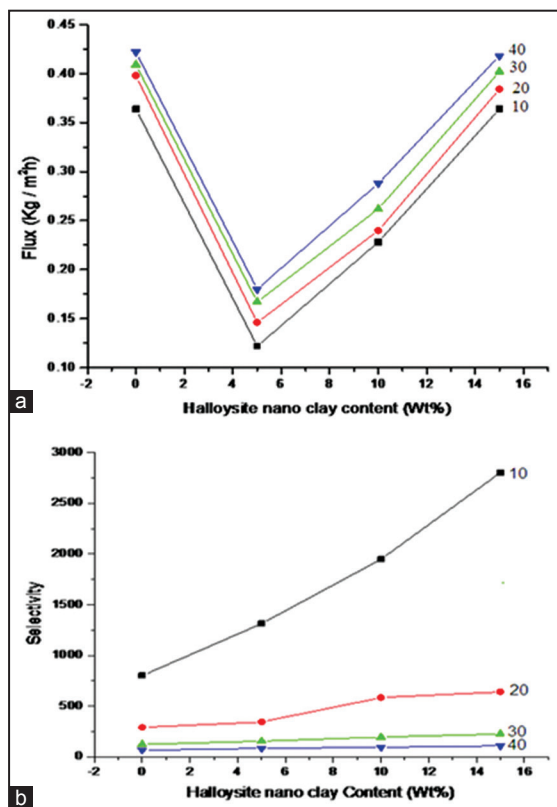


**Figure 9:** (a) Effect of halloysite nanoclay content on flux at different wt% of water in the feed, (b) Effect of Halloysite nanoclay content on selectivity at different wt% of water in the feed.

of water molecules are adsorbed in the hydrophilic clay region, which in turn will get absorbed by the hydrophilic regions of the blend membrane for an easy diffusion through the barrier membrane. Notice that after 5 wt% of clay the flux of clay filled blend membrane is slightly lower than the M1 membrane. Therefore separation takes place due to the selective adsorption of water molecules on to the hydrophilic sites of the clay particles, which will then diffuse through the hydrophilic blend membrane, by inhibiting the transport of organic component (IPA) from the feed mixtures. This further promotes for an increased flux due to increase in driving force. It may be noted that molecular transport occurs due to the faster desorption rate of water molecules on the permeate side. This effect is more beneficial for water transport since water molecules will occupy most of the channels in the hydrophilic regions of the mixed matrix membranes. This also justifies a marked increase in the water selectivity with a recovery of higher amount of water on the permeate side by sacrificing the flux. In any case, the complimentary effects of HNC on water transport will help to improve the membrane performance, thereby offering a high selectivity to water. The selection of clay as filler is helpful to achieve good enhancement of selectivity and flux to the water in the present work.

#### 4. CONCLUSIONS

This investigation clearly demonstrates the effect that by incorporating HNC particles into NaCMC/HPC blend host matrix, it is possible to enhance remarkably the PV performance of the filled blend matrix membranes over that of unfilled NaCMC/HPC blend membrane for IPA dehydration. However, higher loadings of HNC particles rendered the NaCMC/HPC matrix more rigid with a loss of flux but giving increased selectivity to water. Membrane characterization by FTIR, DSC, TGA, SEM, and XRD measurements revealed an adequate thermal and mechanical stability as well as surface free energy of the membranes, which are essential for PV dehydration above the ambient temperature.

#### 5. REFERENCES

1. R. J. Young, P. A. Lovell, (2011) *Introduction to Polymers*, 3<sup>rd</sup> ed. Boca Raton, FL: CRC Press, p591-622.
2. G. Cao, Y. Wang, (2011) *Nanostructures and Nano Materials: Synthesis, Properties, and Applications*, 2<sup>nd</sup> ed. Singapore: World Scientific, p61-142.
3. K. M. Dean, E. Petinakis, L. Yu, (2011) Biodegradable thermoplastic starch/poly (vinyl alcohol) nanocomposites with layered silicates. In: V. Mittal, (Ed.), *Nanocomposites with Biodegradable Polymers: Synthesis, Properties and Future Perspectives*, Oxford, UK: Oxford University Press, p58-70.
4. M. Liu, B. Guo, M. Du, D. Jia, (2007) Drying induced aggregation of halloysite nanotubes in polyvinyl alcohol/halloysite nanotubes solution and its effect on properties of composite film, *Applied Physics A*, **88**: 391-395.
5. E. Joussein, S. Petit, J. Churchman, B. Theng, D. Righi, B. Delvaux, (2005) Halloysite clay minerals-a review, *Clay Miner*, **40**: 383-426.
6. P. Rathi, (2007) Soy protein based nanophase reins for green composites, A Project Report. Ithaca, NY: Cornell University, p13-18.
7. M. Liu, B. Guo, M. Du, X. Cai, D. Jia, (2007) Properties of halloysite nanotube-epoxy resin hybrids and the interfacial reactions in the systems, *Nanotechnology*, **18(45)**: 455703 (1-9).
8. Y. Ye, H. Chen, J. Wu, L. Ye. (2007) High impact strength epoxy nanocomposites with natural nanotubes, *Polymer*, **48**: 6426-6433.
9. S. Deng, J. Zhang, L. Ye, J. Wu, (2008) Toughening epoxies with halloysite nanotubes, *Polymer*, **49**: 5119-5127.
10. N. Ning, Q. Yin, F. Luo, Q. Zhang, R. Du, Q. Fu, (2007) Crystallization behavior and mechanical properties of polypropylene/halloysite composites, *Polymer*, **48**: 7374-7384.
11. M. Du, B. Guo, D. Jia. (2006) Thermal stability and flame retardant effect of halloysite nanotubes on poly (propylene), *European Polymer Journal*, **42**: 1362-1369.

12. D. C. O. Marney, L. J. Russell, D. Y. Wu, T. Nguyen, D. Cramm, N. Rigopoulos, N. Wright, M. Greaves, (2008) The suitability of halloysite nanotubes as a fire retardant for nylon 6, *Polymer Degradation and Stability*, **93**: 1971-1978.
13. M. Du, B. Guo, Y. Lei, M. Liu, D. Jia, (2008) Carboxylated butadiene-styrene rubber/halloysite nanotube nanocomposites: interfacial interaction and performance, *Polymer*, **49**: 4871-4876.
14. B. Guo, Y. Lei, F. Chen, X. Liu, M. Du, D. Jia, (2008) Styrene-butadiene rubber/halloysite nanotubes nanocomposites modified by methacrylic acid, *Applied Surface Science*, **255**: 2715-2722.
15. P. Pasbakhsh, H. Ismail, M.N.A. Fauzi, A.A. Bakar, (2010) EPDM/modified halloysite nanocomposites, *Applied Clay Science*, **48**: 405-413.
16. R. Nakamura, A. N. Netravali, M. Hosur, (2012) Effect of halloysite nanotubes on interfacial property between carbon fiber and epoxy resin, *Journal of Adhesion Science and Technology*, **26**: 1295-1312.
17. R. Nakamura, A. N. Netravali, A. B. Morgan, M. R. Nyden, J. W. Gilman, (2012) Effect of halloysite nanotubes on mechanical properties and flammability of soy protein based green composites, *Fire and Materials*, **37**: 75-90.
18. S. Y. Nam, H. J. Chun, Y. M. Lee, (1999) Pervaporation separation of water-isopropanol mixture using carboxymethylated poly (vinyl alcohol) composite membranes, *Journal of Applied Polymer Science*, **72**: 241-249.
19. G. Y. Moon, R. Pal, R. Y. M. Huang, (1999) Novel two-ply composite membranes of chitosan and sodium alginate for the pervaporation dehydration of isopropanol and ethanol, *Journal of Membrane Science*, **156**: 17-27.
20. Y. L. Liu, Y. H. Su, K. R. Lee, J. Y. Lai, (2005) Crosslinked organic-inorganic hybrid chitosan membranes for pervaporation dehydration of isopropanol-water mixtures with a long-term stability, *Journal of Membrane Science*, **251**: 233-238.
21. Y. M. Lee, S. Y. Nam, B. R. Lee, D. J. Woo, K. H. Lee, J. M. Won, B. H. Ha, (1996) Dehydration of alcohol solutions through crosslinked chitosan composite membranes; Preparation of chemically crosslinked chitosan composite membranes and ethanol dehydration, *Membrane (Korea)*, **20**: 37-43.
22. T. M. Aminabhavi, R. S. Khinnavar, S. B. Harogopad, U. S. Aithal, Q.T. Nguyen, K. C. Hansen, (1994) Pervaporation separation of organic-aqueous and organic-organic binary mixtures, *Journal of Macromolecular Science, Reviews in Macromolecular Chemistry and Physics*, **34**: 139-204.
23. S. D. Bhat, T. M. Aminabhavi, (2007) Pervaporation separation using sodium alginate and its modified membranes-a review, *Separation and Purification Reviews*, **36**: 203-229.
24. I. Blume, J. G. Wijmans, R. W. Baker, (1990) The separation of dissolved organics from water by pervaporation, *Journal of Membrane Science*, **49**: 253-286.
25. P. Shao, R. Y. M. Huang, (2007) Polymeric membrane pervaporation, *Journal of Membrane Science*, **287**: 162-179.
26. J. A. Menjivar, (1986) Use of gelation theory to characterize metal cross-linked polymer gels, *Advances in Chemistry Series*, **213**: 209-226.
27. P. Liu, M. Zhai, J. Li, J. peng, J. Wu, (2002) Radiation preparation and swelling behavior of sodium carboxy methyl cellulose hydrogels, *Radiation Physics and Chemistry*, **63**: 525-528.
28. O. H. Lin, R. N. Kumar, H. D. Rozman, Mohd. A. M. Noor, (2005) Grafting of sodium carboxymethylcellulose (CMC) with glucidylmetha crylate and development of UV curable coating from CMC-g-GMA induced by cationic photoinitiators, *Carbohydrate Polymers*, **59**: 57-69.
29. Y. Cao, H. Li, (2002) Interfacial activity of novel family of polymeric surfactants, *European Polymer Journal*, **38**: 1457-1463.
30. P. G. Bowler, S. A. Jones, B. J. Davies, E. Coyle, (1999) Infection control properties of some wound dressing, *Journal of Wound Care*, **8**: 499-502.
31. C. K. Ryan, H. C. Sax, (1995) Evaluation of a carboxymethyl cellulosesponge for prevention of postoperative adhesion, *The American Journal of Surgery*, **169**: 154-160.
32. M. G. Cascone, L. Di Silvio, B. Sim, S. Downes, (1994) Collagen and hyaluronic acid based polymeric blends as drug delivery systems for the release of physiological concentrations of growth hormone, *Journal of Materials Science*, **5**: 770-774.
33. L. M. Weiner, L. A. Kotkoskie, (1999) *Excipient Toxicity and Safety*, London: Taylor & Francis.
34. R. D. Hagenmaier, P. E. Shaw, (1990) Moisture permeability of edible films made with fatty acid and (hydroxypropyl) methylcellulose, *Journal of Agricultural and Food Chemistry*, **38**: 1799-1803.
35. J. F. Hanlon, (1992) *Handbook of Package Engineering*, Lancaster, UK: Technomic.
36. C. X. Xu, R. Y. Chen, X. Zheng, X. H. Huang, Z. X. Chen, X. H. Hung, Z. Chen, (2006) Preparation of CS-CMC polyelectrolyte membrane and its application to electro-generation of FeO<sub>4</sub><sup>2-</sup>, *Acta Chimica Sinica*, **64**: 784-788.
37. H. J. Xiao, C. L. Hou, S. B. Guan, Y. P. Liu, (2006) Preparation and evaluation of chitosan – Carboxymethyl cellulose membrane for prevention of postoperative intestinal adhesion:

- An experimental study. *Academic Journal of Second Military Medical University*, **27**: 755-759.
38. C. Venkata Prasad, B. Yerri Swamy, H. Sudhakar, T. Sobharani, K. Sudhakar M. C. S. Subha, K. Chowdoji Rao, (2011) Preparation and characterization of 4A Zeolite-filled mixed matrix membranes for pervaporation dehydration of isopropyl alcohol, *Journal of Applied Polymer Science*, **121**: 1521-1529.
  39. H. Sudhakar, K. Chowdoji Rao, S. Sridhar, (2010) Effect of multi-walled carbon nanotubes on pervaporation characteristics of chitosan membrane, *Designed Monomers and Polymers*, **13**: 287-299.
  40. K. W. Boddeker, (1990) Terminology in pervaporation, *Journal of Membrane Science*, **51**: 259-272.
  41. A. P. Rokhade, S. A. Agnihotri, S. A. Patil, N. N. Mallikarjuna, P. V. Kulkarni, T. M. Aminabhavi, (2006) Semi-interpenetrating polymer network microspheres of gelatin and sodium carboxymethyl cellulose for controlled release of ketorolac tromethamine, *Carbohydrate Polymers*, **65**: 243-252.
  42. S. G. Adoor, B. Prathab, L. S. Manjeshwar, T. M. Aminabhavi, (2007) Mixed matrix membranes of sodium alginate and poly(vinyl alcohol) for pervaporation dehydration of isopropanol at different temperatures, *Polymer*, **48**: 5417-5430.
  43. M. D. Kur Kuri, U. S. Toti, T. M. Aminabhavi, (2003) Pervaporation separation of water and dioxane mixtures with sodium alginate-g-polyacrylamide copolymeric membranes, *Journal of Applied Polymer Science*, **89**: 300-305.
  44. M. D. Kurkuri, U. S. Toti, T. M. Aminabhavi, (2002) Synthesis and characterization of blend membranes of sodium alginate and poly (vinyl alcohol) for the pervaporation separation of water + Isopropanol mixtures, *Journal of Applied Polymer Science*, **86**: 3642-3651.
  45. K. V. Sekharnath, U. Sajankumarji Rao, Y. Maruthi, M. N. Prabhakar, M. C. S. Subha, K. Chowdoji Rao, J. Song, (2014) Pervaporation separation of water-isopropanol mixture using MFI-24Q zeolite incorporated blend (NaAlg and HPC) membranes, *International Journal of Scientific & Technology Research*, **3**: 219-227.
  46. X. Qiao, T. S. Chung, (2005) Fundamental characteristics of sorption, swelling, and permeation of P84 co-polyimide membranes for pervaporation dehydration of alcohols, *Industrial and Engineering Chemistry Research*, **44**: 8938-8943.
  47. S. B. Teli, G. S. Gokali, T. M. Aminabhavi, (2007) Novel sodium alginate-poly(N-isopropylacrylamide) semi-interpenetrating polymer network membranes for pervaporation separation of water + ethanol mixtures, *Separation and Purification Technology*, **56**: 150-157.
  48. K. V. Sekharnath, S. Siraj, U. Sajankumarji Rao, P. Sudhakar, Y. Maruthi, P. Kumarbabu, M.S.C. Subha, K. Chowdoji Rao, (2014) Phosphomolybdic acid embedded PVA-Pectin blend membranes for pervaporation dehydration of isopropanol and water, *Advances in Polymer Science and Technology: An International Journal*, **4**: 60-68.
  49. J. G. Wijmans, R. W. Baker, (1995) The solution-diffusion model: A review, *Journal of Membrane Science*, **107**: 1-21.

**\*Bibliographical Sketch**



Dr. K.V. Sekharnath has graduated from AVR-Degree college Tadipatri and M.Sc chemistry from Sir C.V. Raman college affiliated to S.K.University, He has obtained his Ph.D degree from S.K.University under the guidance of Prof. (Mrs).M.C.S.SUBHA, Dept.of chemistry, S.K.University. He has published 10 research papers in reputed International journals and also presented his papers in 8 National & International conferences/ seminars. He has also teaching experince Asst.professor Chemistry in Tadipatri Engineering College, Tadipatri, A.P